Gas-Phase f-Element Organometallic Chemistry: Reactions of Cyclic Hydrocarbons with Th^+, U^+, ThO^+, UO^+, and Lanthanide Ions, Ln^+

John K. Gibson

Chemical and Analytical Sciences Division, Oak Ridge National Laboratory, P.O. Box 2008, Oak Ridge, Tennessee 37831-6375

Received March 13, 1997[⊗]

The extent of reaction of metal ions, M^+, with organic molecules depends upon the electronic structure of the metal ion; in particular, the degree to which laser-ablated lanthanide ions, Ln^+, dehydrogenate hydrocarbons is known to reflect the energy needed to excite ground state Ln^+ to a divalent configuration. Reported here are gas-phase reactions of Ln^+ and AnO_n^+ (An = Th or U; $n = 0$ or 1) with C_6 and C_8 cyclic hydrocarbons. The reactivities of Ln^+ with c-C_8H_{8+2m} ($m = 0$, 2, or 4) were consistent with previous results for $Ln^+ +$ c-C_6H_{6+2m}, in that the relative dehydrogenation efficiencies reflected the metal ion electronic structure and excitation energy. Additionally, the relatively strong bonding between Ln^+ and cyclooctatetraene (COT) was manifested as abundant condensation adduct, Ln^+−COT. The dehydrogenation reactivities of Th^+ and U^+ with both C_6 and C_8 cyclic hydrocarbons were found to be comparable to that of Ce^+, the most reactive Ln^+, consistent with divalent An^+ electronic configurations and a dehydrogenation mechanism initiated by oxidative insertion of An^+ into a C−H bond. The most conspicuous discrepancy between the actinide and lanthanide results was the significant dehydrogenation reactivities of the AnO^+, this in sharp contrast to essentially inert behavior of all LnO^+ studied. In view of the similarity between Ce and Th, the substantial reactivity of ThO^+ in light of the inert behavior of CeO^+ is particularly intriguing and suggests a central role of the metal center in the dehydrogenation process. The activity of the AnO^+ may reflect the distinctive nature of the 5f valence orbitals and could be partly attributable to relativistic effects. An ancillary result of the present investigation was the identification of several metal oxide clusters comprising uranium in multiple valence states.

Introduction

The study of gas-phase reactions of metal ions (M^+) with various organic substrates has developed into an important field of investigation in recent years, reflecting the ability to probe fundamental chemistry and enhance understanding of condensed-phase processes such as catalysis.[1,2] Whereas the initial focus was primarily on prevalent d-block transition elements, particularly those in the first row, the f-block lanthanide (Ln) and actinide (An) elements have received appreciable attention since the initial lanthanide studies by Schilling and Beauchamp[3] revealed marked variations in the reactivities of different Ln^+, this in contrast to the generally quite similar condensed-phase organolanthanide chemistries exhibited across the series.[4] Subsequent studies[5−7] have substantiated the initial proposal[3] that discrepant Ln^+ reactivities reflect the energy necessary to excite the ground state ion to a divalent configuration with two non-4f valence electrons which enables insertion into a C−H bond to yield a C−Ln^+−H activated intermediate.

The primary techniques for studying hydrocarbon activation by metal ions are FTICR-MS[6] and guided ion beam mass spectrometry.[5] Recent results from our laboratory[8] demonstrated that the laser ablation molecular beam (LAMB) method described by Sato et al.[9] can also be used to coherently differentiate the electronic structures and excitation energies of Ln^+ as reflected in their dehydrogenation/complexation reactions with cyclic hydrocarbons, this despite that nascent laser-ablated Ln^+ possess substantial kinetic energies that may promote endothermic processes.[5,9] An important implication of the consistent differentiation between Ln^+ reactivities using the LAMB technique was that the internal energies of the laser-ablated metal ions at the time of their encounter with the neutral reactant (i.e., ≥ 1 μs after ablation) were insufficient to obscure ground state electronic structures and excitation energies.

Organoactinide chemistry was inaugurated with the synthesis of the remarkably stable bis-π-cyclooctatetraene (COT)−uranium[10] and −thorium[11] "actinocenes"

[⊗] Abstract published in *Advance ACS Abstracts*, August 15, 1997.

(1) Eller, K.; Schwarz, H. *Chem. Rev.* **1991**, *91*, 1121−1177.
(2) Freiser, B. S. *J. Mass Spectrom.* **1996**, *31*, 703−715.
(3) Schilling, J. B.; Beauchamp, J. L. *J. Am. Chem. Soc.* **1988**, *110*, 15−24.
(4) Schumann, H.; Genthe, W. In *Handbook on the Physics and Chemistry of Rare Earths*; Gschneidner, K. A., Jr., Eyring, L., Eds.; Elsevier: New York, 1984; Vol. 7, pp. 445−571.
(5) Sunderlin, L. S.; Armentrout, P. B. *J. Am. Chem. Soc.* **1989**, *111*, 3845−3855.
(6) Yin, W. W.; Marshall, A. G.; Marcalo, J.; Pires de Matos *J. Am. Chem. Soc.* **1994**, *116*, 8666−8672.
(7) Cornehl, H. H.; Heinemann, C.; Schroder, D.; Schwarz, H. *Organometallics* **1995**, *14*, 992−999.
(8) Gibson, J. K. *J. Phys. Chem.* **1996**, *100*, 15688−15694.
(9) Higashide, H.; Oka, T.; Kasatani, K.; Shinohara, H.; Sato, H. *Chem. Phys. Lett.* **1989**, *163*, 485−489.
(10) Streitwieser, A., Jr.; Muller-Westerhoff, U. *J. Am. Chem. Soc.* **1968**, *90*, 7364.

S0276-7333(97)00205-7 CCC: $14.00

by Streitwieser et al. Subsequently, many π-bonded[12] and σ-bonded[13] organoactinides have been prepared for U and Th. Interest in organoactinide chemistry is partly motivated by the role of relativistic effects and 5f bonding and the apparent intermediacy of the actinides between the largely covalent d-block transition metals and ionic lanthanides.[14] Initial gas-phase organoactinide studies of U^+ [15] and Th^+ [16] have focused on the activation of small hydrocarbons by bare An^+ and indicated reactivities at least as high as for the most reactive Ln^+ in accord with a rate-controlling step involving C−H or C−C activation by insertion of divalent M^+. Since both Th^+ and U^+ exhibit ground (Th^+) or very low-lying (U^+) electronic configurations comprising two non-5f valence electrons, their reactivities do not illuminate the potential role of 5f orbitals in bond activation.[16]

Condensed-phase lanthanide−arene[17] and lanthanide−COT[18] complexes have been prepared, including divalent Ln^{2+}−COT^{2-} for Ln = Eu and Yb.[19] Several Ln form trivalent compounds of the type COT^{2-}−Ln^{3+}−X^- [20] and K^+−{COT^{2-}−Ln^{3+}−COT^{2-}},[21] but cerrocene is the only known genuine lanthanocene.[22] Theoretical[23] and experimental[24] studies of cerrocene have suggested trivalent Ce, in contrast to tetravalent Th in thoracene. The strong and unique M^{n+}−COT^{2-} bond[23] contrasts with electrostatic M^{n+}−arene bonding;[25] it is appropriate to extend gas-phase organometallic studies to COT, particularly with actinides and lanthanides where COT is central in condensed-phase organometallic chemistry.[26] Conventional f-element organometallic chemistry is constrained by the reactivity of the metal center, and bulky ligands such as Cp* are often exploited to sterically protect a reactive low-valent metal center. Low-valent organolanthanide chemistry is primarily limited to Eu, Yb, and Sm.[27] In contrast, low-pressure gas-phase organometallic chemistry accesses labile complexes such as Ln^+−benzene.

An important consideration in gas-phase ion chemistry regards ligand effects on metal center reactivity. Oxide ions, MO^+, of late transition metals typically transfer an O atom to organic substrates but the M−O bond of early transition and lanthanide elements is rarely severed.[28] For LnO^+, the two available active (non-4f) valence electrons at the metal center are engaged in the strong Ln=O bond and these species are essentially inert.[28] In contrast, pentavalent V retains two free valence electrons in VO^+ and the metal center of this oxide ion is comparably reactive to bare V^+.[29] A species such as $^\bullet Y^+-CH_3$ represents the intermediate scenario of a single-valence electron at the metal center—there C−H activation may proceed through a multicenter intermediate.[30] The light actinides form strong An−O bonds,[31] and oxidation of an organic substrate by AnO^+ is not feasible. Beyond Ac, the AnO^+ present one or more 5f and/or 5d/6s valence electrons at the metal center which may participate in C−H or C−C bond activation. It is of interest to determine reactivities of AnO^+ as the number of valence electrons increases across the series while concurrently the 5f electrons become increasingly contracted and unsuited to chemical interaction.

We report here the results of the extension of gas-phase organolanthanide chemistry to the study of Ln^+ + cyclo-C_8 hydrocarbon reactions and compare the results with those reported previously for Ln^+ with other organic substrates. Results for reactions of U^+ and Th^+ with both cyclic C_6 and C_8 hydrocarbons are also reported and compared with those for Ln^+ in the context of dehydrogenation mechanistics. In addition, dehydrogenation by UO^+ and ThO^+ is described and discussed in view of the effect of the oxygen ligand on the electronic structure of the metal center and its consequent reactivity and the contrastingly inert character of LnO^+.

An ancillary outcome was the laser ablation synthesis of gaseous metal oxide cluster ions incorporating uranium. The condensed-phase oxide chemistry of U is conspicuously complex,[32] reflecting the availability of multiple oxidation states. Variable uranium valences have also been manifested in gas-phase $U_mO_n^+$ clusters.[33] We report uranium oxide clusters identified in the course of the present investigation and compare/contrast these results with those obtained previously for lanthanide oxides.[34]

Experimental Section

i. Procedures. The laser ablation mass spectrometer[35] and its application to the investigation of reactions of metal ions with organic molecules[8] have been described previously. A reactant gas is leaked into the trajectory of ions which have been ablated from a solid target by a XeCl excimer laser (λ =

(11) Streitwieser, A., Jr.; Yoshida, N. *J. Am. Chem. Soc.* **1969**, *91*, 7528.
(12) Marks, T. J.; Streitwieser, A., Jr. In *The Chemistry of the Actinide Elements*; 2nd ed.; Katz, J. J., Seaborg, G. T., Morss, L. R., Eds.; Chapman and Hall: New York, 1986; Vol. 2, pp 1547−1587.
(13) Marks, T. J. In *The Chemistry of the Actinide Elements*; 2nd ed.; Katz, J. J., Seaborg, G. T., Morss, L. R., Eds.; Chapman and Hall: New York, 1986; Vol. 2, pp 1588−1628.
(14) Pepper, M.; Bursten, B. E. *Chem. Rev.* **1991**, *91*, 719−741.
(15) Heinemann, C.; Cornehl, H. H.; Schwarz, H. *J. Organomet. Chem.* **1995**, *501*, 201−209.
(16) Marcalo, J.; Leal, J. P.; Pires de Matos, A. P. *Int. J. Mass Spectrom. Ion Processes* **1996**, *157/158*, 265−274.
(17) Deacon, G. B.; Shen, Q. *J. Organomet. Chem.* **1996**, *511*, 1−17.
(18) Edelman, F. T. *Angew. Chem., Int. Ed. Engl.* **1995**, *34*, 2466−2488.
(19) Hayes, R. G.; Thomas, J. L. *J. Am. Chem. Soc.* **1969**, *91*, 6876.
(20) Schumann, H.; Rosenthal, E. C. E.; Winterfeld, J.; Weimann, R.; Demtschuk, J. *J. Organomet. Chem.* **1996**, *507*, 287−289.
(21) Hodgson, K. O.; Mares, D. F.; Starks, D. F.; Streitwieser, A., Jr. *J. Am. Chem. Soc.* **1973**, *95*, 8650−8658.
(22) Greco, A.; Cesca, S.; Bertolini, G. *J. Organomet. Chem.* **1976**, *113*, 321.
(23) Dolg, M.; Fulde, P.; Stoll, H.; Preuss, H.; Chang, A.; Pitzer, R. M. *Chem. Phys.* **1995**, *195*, 71−82.
(24) Edelstein, N. M.; Allen, P. G.; Bucher, J. J.; Shuh, D. K.; Sofield, C. D. *J. Am. Chem. Soc.* **1996**, *118*, 13115−13116.
(25) Bauschlicher, C. W. Jr.; Partridge, H.; Langhoff, S. R. *J. Phys. Chem.* **1992**, *96*, 3273−3278.
(26) Cotton, F. A.; Wilkinson, G. *Advanced Inorganic Chemistry*; 5th ed.; John Wiley & Sons, New York, 1988; pp 968−997, 1177−1179.
(27) Evans, W. J. *Polyhedron* **1987**, *6*, 803−835.
(28) Schroder, D.; Schwarz, H. *Angew. Chem., Int. Ed. Engl.* **1995**, *34*, 1973−1995.
(29) Jackson, T. C.; Carlin, T. J.; Freiser, B. S. *J. Am. Chem. Soc.* **1986**, *108*, 1120−1126.
(30) Huang, Y.; Hill, Y. D.; Freiser, B. S. *J. Am. Chem. Soc.* **1991**, *113*, 840−845.
(31) Haire, R. G. *J. Alloys Cmpds.* **1994**, *213/214*, 185−190.
(32) Weigel, F.; Hoekstra, H. R. In *The Chemistry of the Actinide Elements*; 2nd ed.; Katz, J. J., Seaborg, G. T., Morss, L. R., Eds.; Chapman and Hall: New York, 1986; Vol. 1, pp 256−280.
(33) Tench, R. J.; Balooch, M.; Bernardez, L.; Allen, M. J.; Siekhaus, W. J.; Olander, D. R.; Wang, W. In *Laser Ablation for Materials Synthesis*; Materials Research Society Proceedings 191; Paine, D. C., Bravman, J. C., Eds.; Materials Research: Pittsburgh, 1990; pp 85−91.
(34) Gibson, J. K. *J. Phys. Chem.* **1994**, *98*, 11321−11330.
(35) Gibson, J. K. *J. Phys. Chem.* **1994**, *98*, 6063−6067.

308 nm); the resulting positive ions—both those remaining unreacted and those resulting from ion−molecule reactions—are determined with a reflectron time-of-flight mass spectrometer. The reactant gas pressure was not determined (estimated as $\gg 10^{-3}$ Pa) but was similar for all experiments and was sufficient to react with up to ∼50% of the most reactive ions (e.g., W^+). The time delay between the laser pulse and product ion injection into the mass spectrometer could be varied, and ions were typically detectable within a delay range of ∼10−100 μs; optimal reaction product detection/resolution was generally achieved for delays of 30−40 μs, and the reported results were obtained using this range. Ion injection occurred ∼3 cm from the target so that a delay of 30 μs sampled ions with an average velocity of ∼1 km s^{-1}, which corresponds to a kinetic energy of ∼1.2 eV (∼120 kJ mol^{-1}) for $^{238}U^+$. The laser was attenuated to provide ∼0.5−10 mJ on the target, focused to a spot of ∼0.5 mm^2; assuming the nominal laser pulse width of 15 ns, this corresponds to irradiances of $\sim 10^7-10^8$ W cm^{-2}. Most targets supplied abundant ions using $\sim 10^7$ W cm^{-2}, but highly refractory materials such as tungsten required $\sim 10^8$ W cm^{-2}.

ii. Materials. Several ablation targets were used in the present study. The starting materials were commercial products, most with purities of at least 99.8%; the exceptions were UTe_2 and $ThSi_2$, which were 99.5% pure, and the depleted uranium metal turning, which was 99.7% pure. The "single-component" targets were used as-supplied. The "alloy" targets were prepared by arc melting the respective pure metals as described previously.[8] The "copper dispersion" targets were prepared by room-temperature compression of physical mixtures of the actinide/lanthanide-containing constituents in a copper matrix using a small manual pellet press (Parr Model 2811 with a 3 mm diameter die); this target preparation method is versatile and will be applicable to transuranic materials handled in a laboratory glove box. Copper was identified as a suitable matrix since it forms dense pellets under moderate pressures and produced minor amounts of Cu^+. The "**CuTbEu**" target generated ion signals (expressed as millivolts) of ∼500 for Eu^+, ∼100 for Tb^+, and only ∼1 for Cu^+. (In contrast, the yield of Zn^+ was comparable to that of Tb^+ for a 3% Eu/3% Tb/94% Zn target.) The total mass of a typical copper pellet target was ∼0.1 g. Cross-contamination between sequentially prepared alloy or copper pellet targets was occasionally manifested by the appearance of contaminant M^+ in mass spectra (particularly for volatile and/or easily ionized contaminants); contaminants that produced sufficient ion intensities to allow for the study of their reactivities are indicated below in parentheses. The aggregate target compositions are expressed in mole percent. The abbreviated designation subsequently used to identify each target is indicated in bold (e.g., "**CuCeTh(U)**"); constituents omitted from these designations either produced minor ion yields or were not relevant to the present study. Hydrated uranyl acetate, $UO_2(C_2H_3O_2)_2{\cdot}2H_2O$, is denoted below as "$UO_2AC_2$."

Single-Component Targets: $CeSi_2$; **Yb^o**; **Tb^o**; **Ho^o**; **W^o**; **U^o_t** (depleted metal turning); **U^o_w** (wire).

Alloy Targets: $Tb_{50}Ho_{50}$, "**TbHo**"; $Dy_{65}Tm_{35}$, "**DyTm**"; $Gd_{64}Lu_{36}$(Tm), "**GdLuTm**"; $Ti_{30}Zr_{30}Hf_{40}$, "**TiZrHf**"; $Cu_{86}Pr_7Sm_8$, "**CuPrSm**".

Copper Dispersion Targets: $Cu_{94}[TbO_{3/2}]_3[EuO_{3/2}]_3$, "**CuTbEu**"; $Cu_{90}Zr_3[CeSi_2]_3[ThSi_2]_4$(U), "**CuCeTh(U)**"; $Cu_{91}[CeSi_2]_3[ThO_2]_3[UO_2AC_2]_2$, "**CuCeThU**"; $Cu_{90}Mo_3[CeSi_2]_4[UTe_2]_4$, "**CuCeU**"; $Cu_{89}Nb_3Ho_2[ThSi_2]_2[UTe_2]_4$, "**CuHoThU**".

A small (<1 mL) volume of the organic reactant was placed into a vial attached to the leak valve leading to the gas inlet inside of the ion source region. At least one freeze−evacuation−thaw cycle was performed prior to use. The benzene was standard analytical grade reagent. The other organics were stock commercial products (Aldrich) with the following purities: 99% cyclohexene; 99% cyclooctane (COA); 99% 1,5-cyclooctadiene (COD); and 98% 1,3,5,7-cyclooctatetraene (COT).

Table 1. Yields from $Ln^+ + COT$[a]

	$M^+-C_8H_8$	$M^+-C_8H_6$
TbHo		
Tb^+	0.5	0.6
Ho^+	0.8	0.5
CuTbEu		
Eu^+	0.7	*n*
Tb^+[b]	(<3)	*n*
CuPrSm		
Pr^+	0.3	0.4
Sm^+	0.3	(<0.2)[c]
DyTm		
Dy^+	0.2	(<0.02)
Tm^+	0.2	(<0.02)
GdLuTm		
Gd^+	0.9	*n*
Lu^+	0.9	*n*
Tm^+	0.9	*n*
TiZrHf		
Ti^+	0.5	0.2

[a] Yield as percent of parent ion intensity (I): yield$[M^+-C_8H_h] = \{I[M^+-C_8H_h]/I[M^+]\} \times 100$. Values in parentheses are limits for unobserved products; *n*, not observed. Coablated M^+ are grouped together. Condensation and dehydrogenation products are reported; products of C−C bond cleavage (abundant for Ti^+/ Zr^+/ Hf^+) are omitted. Results are for $t_d = 30-40$ μs. [b] Very little Tb^+ ($I[Tb^+] \ll I[Eu^+]$). [c] Difficult to discern small concentration of dehydrogenation product for polyisotopic Sm.

Results and Discussion

Primary results are summarized in Tables 1−3 and representative mass spectra are shown in Figures 1−5. The tabulated results give the relative yields of the observed products which resulted from non-reactive condensation, eq 1 with $e = 0$; or dehydrogenation accompanied by complexation, eq 1 with $e \geq 1$.

$$MO_n^+ + \text{cyclo-}C_cH_{c+2m} \rightarrow MO_n^+-C_cH_{c+2m-2e} + eH_2 \quad (1)$$

For the lanthanides (M = Ln), no reaction product ions were ever observed for the LnO^+ so that only results for the bare Ln^+ ($n = 0$) are reported. For M = U or Th, products were identified for the AnO^+ (and occasionally for UO_2^+) as well as for the bare An^+. In addition to the condensation and dehydrogenation products included in the tables, some C−C cleavage products were apparent, particularly for reactive species such as U^+ and W^+; for example, U^+ eliminated C_2H_2 and C_2H_4 from COD (Figure 4). The focus of the discussion is on the dehydrogenation products as most M^+ effected some H_2 loss and those results were most amenable to coherent comparison of reactivities.

The percent yields are expressed as the measured product ion intensity relative to the concurrently measured reactant ion intensity: yield$[MO_n^+-C_cH_{c+2m-2e}] \equiv I[MO_n^+-C_cH_{c+2m-2e}]/I[MO_n^+] \times 100$. The comparative results are most reliable for ions simultaneously coablated from the same target, which are grouped together in the tables; comparisons between reaction yields for ions studied in separate experiments using different targets are considered definitive for yield differences of at least 1 order of magnitude.

The representative mass spectra in Figures 1−3 include separate segments comprising the parent (reactant) ion peaks (MO_n^+) and the product ion peaks at higher mass; the more sensitive intensity scales for the product ion segments are indicated by scale markers. The bottom linear abscissa scales indicate the measured ion flight times; the top nonlinear scales indicate the

Table 2. Yields from MO_n^+ + cyclo-C_6H_h (M = Th, U, or Ln)[a]

	$MO_n^+-C_6H_6$	$MO_n^+-C_6H_4$
M^+/MO^+ + Benzene		
U^o_w		
U^+	0.03	8
UO^+	0.02	(<0.01)
Tb^o		
Tb^+	0.14	0.25
TbO^+	(<0.01)	(<0.01)
W^o		
W^+	(<2)	44
CuCeTh(U)		
Ce^+ {20}[b]	3	10
CeO^+ {70}	(<0.1)	(<0.1)
Th^+ {2.6}	(<1)	12
ThO^+ {6.6}	1	(<0.3)
U^+ {1.0}	(<2)	~5
M^+/MO^+ + Cyclohexene		
U^o_t[c]		
U^+{19}	3	0.5
UO^+{110}	1.4	(<0.1)
UO_2+{80}	(<0.1)	(<0.1)
U^o_t[c]		
U^+{200}	3	1
UO^+{170}	1.2	(<0.06)
Tb^o		
Tb^+	0.12	0.03
TbO^+	(<0.02)	(<0.02)
W^o		
W^+	5	47
CuCeThU		
Th^+	~6	*n*
ThO^+	~4	*n*
U^+	~6	*n*
UO^+	~2	*n*
CuCeTh(U)		
Ce^+	4	1
CeO^+	(<0.1)	*n*
Th^+	7	3
ThO^+	~6	(<0.2)
U^+	~5	*n*
UO^+	~5	*n*

[a] See footnote *a* of Table 1; also, yield[MO^+-L] = {*I*[MO^+-L]/*I*[MO^+]} × 100. [b] Values in braces are measured reactant ion intensities, *I*[MO_n^+]. [c] The discrepant *I*[U^+] and *I*[UO_2^+] between the **U^o_t** data sets are due to removal of surface oxide.

approximate derived ion masses, *m*/*z* with *z* = 1 (multiply charged ions were rare).

i. Ln^+ + cyclo-C_8H_h. A representative mass spectrum is shown in Figure 1 for the reaction of Pr^+/Sm^+ with COT. The reactions of Ln^+ with COT (Table 1) produced primarily the condensation product Ln^+-COT. A significant observation was that the yields of all Ln^+-COT (as well as Ti^+-COT) condensation products were comparable, in marked contrast to the widely discrepant yields of the dehydrogenation products. This similarity in the COT affinities for different Ln^+ suggests that excitation from the ground state to a divalent configuration was not prerequisite for condensation, consistent with electrostatically bonded Ln^+-COT.

A few Ln^+ + COT reactions additionally resulted in substantial dehydrogenation to produce the $Ln^+-C_8H_6$ complex. Analogy with benzyne would suggest a cyclo-C_8H_6 ligand which includes a C≡C bond. Comparisons of the $Ln^+-C_8H_6$ yields in Table 1 are compatible with the conventional dehydrogenation mechanism initiated by oxidative insertion of divalent M^+ into a C−H bond followed by β-hydrogen elimination.[3] For example, the smaller ground-to-divalent excitation energy for Pr^+ compared with Sm^+ (Table 4) resulted in a greater yield of $Pr^+-C_8H_6$.

Table 3. Yields from MO_n^+ + cyclo-C_8H_h (M = Th, U, or Ln)[a]

	$MO_n^+-C_8H_8$	$MO_n^+-C_8H_6$
MO_n^+ + COT		
U^o_w		
U^+	0.6	0.3
UO^+	*n*	0.8
CuHoThU[b]		
U^+	3	3
UO^+	*n*	5
CuCeThU[b]		
U^+	25	*n*
UO^+	~3	~3
CuCeU		
U^+	1.4	~1
UO^+	*n*	3
CuCeTh(U)		
Ce^+	~0.5	~2
CeO^+	(<0.1)	(<0.1)
Th^+	(<2)	(<2)
ThO^+	*n*	3
MO_n^+ + COD		
U^o_t		
U^+[c]	2.6	0.5
UO^+[c]	0.1	*n*
Ho^o		
Ho^+[c]	1	0.04
Tb^o		
Tb^+	0.5	0.1
W^o		
W^+	0.1	60

[a] See footnote *a* of Table 2. [b] Uranium-containing reactant ions for these targets were dominant; Th^+ was minor. [c] Also 0.6% each of $U^+-C_6H_6$ and $UO^+-C_6H_6$ and 0.06% of $Ho^+-C_6H_6$.

The reactions of Ln^+ with COD proceeded primarily by double dehydrogenation to produce Ln^+-COT in the following yields as defined in Table 1 (targets indicated in braces): Pr^+ = 1, Sm^+ = (<0.1) {**CuPrSm**}; Dy^+ = 2, Tm^+ = 1 {**DyTm**}; Gd^+ = 0.5, Lu^+ = 0.5, Tm^+ = 0.3 {**GdLuTm**}; Yb^+ = (<0.1) {**Yb^o**}; Ce^+ = 3, also $Ce^+-C_8H_6$ = 0.5 {**$CeSi_2$**}; $Ti^+ \approx Zr^+ \approx Hf^+ \approx 20$ (also C−C bond cleavage products) {**TiZrHf**}. The unique stability of Ln^+-COT is demonstrated by the contrasting absence of any Ln^+-COD condensation complexes. The comparative efficiencies of different Ln^+ in dehydrogenating COD indicate C−H activation by insertion of a divalent metal ion; specifically, the relative Ln^+-COT yields from COD generally parallel the excitation energies in Table 4. The group IV transition metals were found to be extremely efficient at dehydrogenation, consistent with previous results;[38] it was suggested that the extraordinary reactivity of Ti^+ may be attributed to the availability of multiple electrons specifically in the valence d-orbital—the ground state configuration of Ti^+, for example is [Ar] $3d^24s^1\ ^4F_{3/2}$.[39] In contrast, the lowest divalent state of most Ln^+ is [Xe] $4f^{n-2}5d^16s^1$—the $4f^{n-2}5d^2$ divalent state might be substantially more reactive. This effectiveness of 5d electrons at C−H activation could account for some apparent anomalies in Ln^+ reactivities;[7,8] for example, the significantly smaller reactivity of Gd^+ compared with Ce^+ might

(36) Martin, W. C.; Zalubas, R.; Hagan, L. *Atomic Energy Levels: The Rare Earth Elements*; Publ. NSRDS-NBS 60; U.S. Dept. of Commerce: Washington, DC, 1978.
(37) Fred, M. S.; Blaise, J. In *The Chemistry of the Actinide Elements*; 2nd ed.; Katz, J. J., Seaborg, G. T., Morss, L. R., Eds.; Chapman and Hall: New York, 1986; Vol. 2, pp 1196−1277.
(38) Tonkyn, R.; Weishaar, J. C. *J. Phys. Chem.* **1986**, *90*, 2305−2308.
(39) Moore, C. E. *Atomic Energy Levels*; Publ. NSRDS-NBS 35; U.S. Dept. of Commerce: Washington, DC, 1971; Vol. 1, pp 273−290.

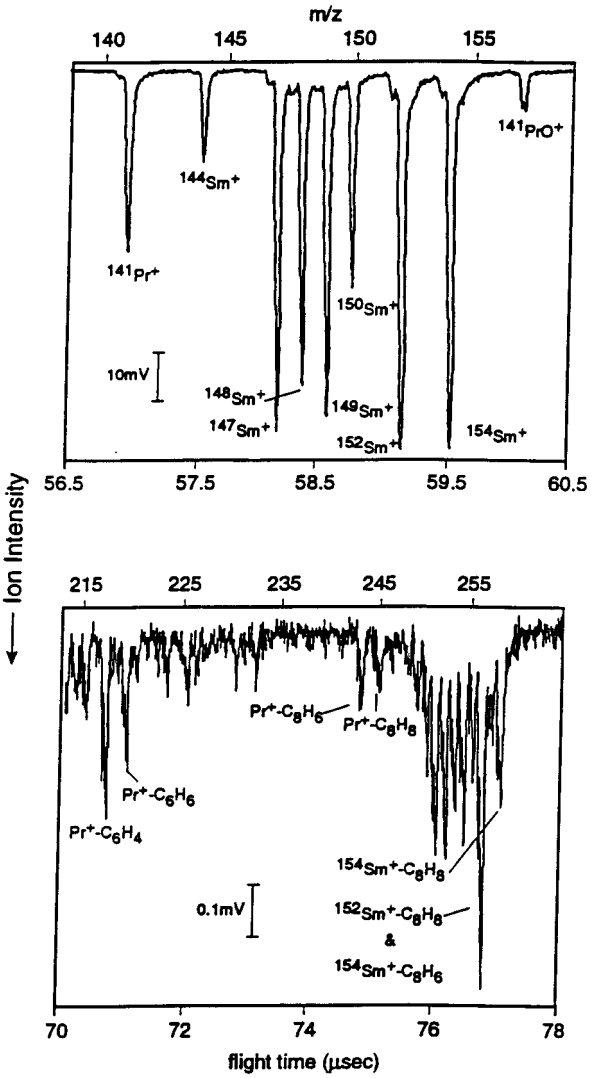

Figure 1. Mass spectrum for the reaction of Pr^+ and Sm^+ (target **CuPrSm**) with cyclooctatetraene (C_8H_8). The bottom abscissa scale gives the measured ion flight times and the nonlinear top abscissa scale represents the derived m/z in atomic mass units; essentially all observed species were +1 ions ($z = 1$). The relative ion intensity scales for different segments of the spectrum are indicated by vertical millivolt (mV) markers.

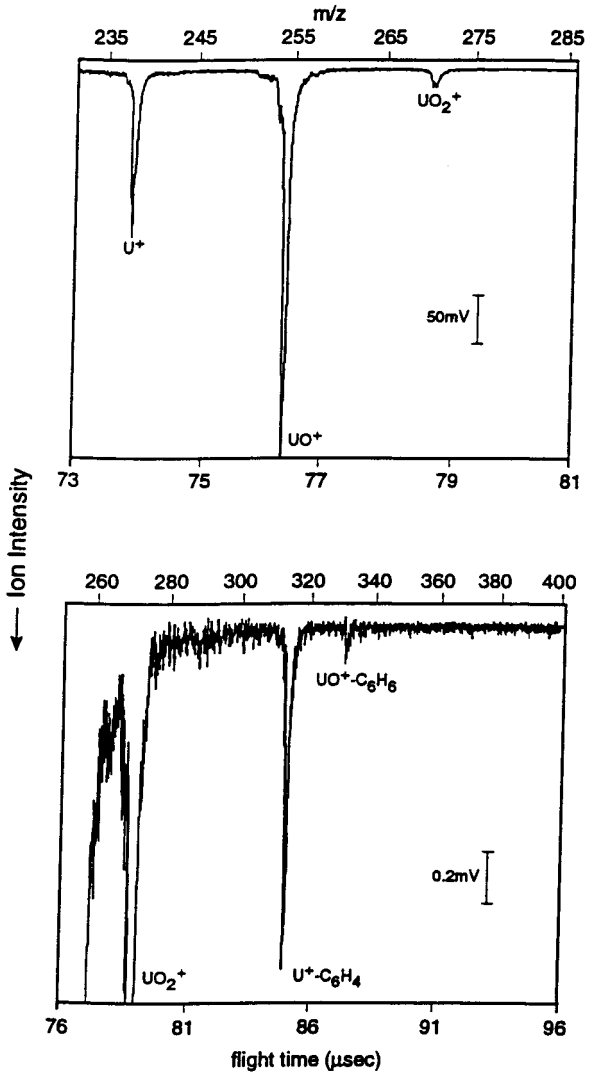

Figure 2. Mass spectrum for the reaction of U^+ and UO^+ (target $\mathbf{U^o_w}$) with benzene (C_6H_6).

reflect that the "divalent" ground state Gd^+ configuration is $4f^75d^16s^1$ whereas that of Ce^+ is $4f^15d^2$, which includes two 5d electrons.[36]

In accord with the generally minor reactivities of Ln^+ [3] (and other M^+ [1]) with saturated hydrocarbons, the reactivities of Ln^+ with COA were minimal, with only Ce^+ generating measurable amounts of the di-, tri-, and tetradehydrogenation complexes—the loss of up to $4H_2$ from COA to form Ce^+-COT was noteworthy.

ii. Reactions of An^+ and AnO^+. Representative actinide mass spectra are shown in Figures 2−4, and main results are compiled in Table 2 for reactions of actinide ions with C_6 substrates and in Table 3 for their reactions with C_8 substrates. In distinct contrast to the inert character of LnO^+ exhibited previously[8] and in the present study, both ThO^+ and UO^+ displayed significant reactivities.

The results for U^0 + benzene showed both U^+ and UO^+ formed some condensation complex; only bare U^+ effected dehydrogenation to give U^+−benzyne. The results for the **CuCeTh(U)** target with benzene are especially revealing. The bare metal ions, Ce^+, Th^+, and U^+ were comparably efficient at dehydrogenating benzene to benzyne. Since both Ce^+ and Th^+ have divalent ground state configurations and U^+ has a divalent configuration only 3 kJ mol^{-1} ($\approx kT$ at 300 K) above ground state, it is reasonable that each should be comparably reactive. The reportedly high reactivity of W^+ [40] is apparent from the results in Table 2 (C−C cleavage products are omitted).

In contrast to the benzene reactions where condensation complexes were sometimes evident as minor products (Table 2), reactions with cyclohexene produced primarily the double dehydrogenation product, MO_n^+−benzene, and secondarily the triple dehydrogenation product, MO_n^+−benzyne. Again, the relative reactivities are consistent with the electronic configurations and excitation energy to achieve a divalent bonding configuration, and the most reactive ion examined was W^+. The two sets of data for uranium metal turning given in Table 2 and shown in Figure 3 represent results for initial ablation of the oxide-contaminated surface—minor U^+ and abundant UO_2^+—and for subsequent ablation

(40) Irikura, K. K.; Beauchamp, J. L. *J. Am. Chem. Soc.* **1991**, *113*, 2769−2770.

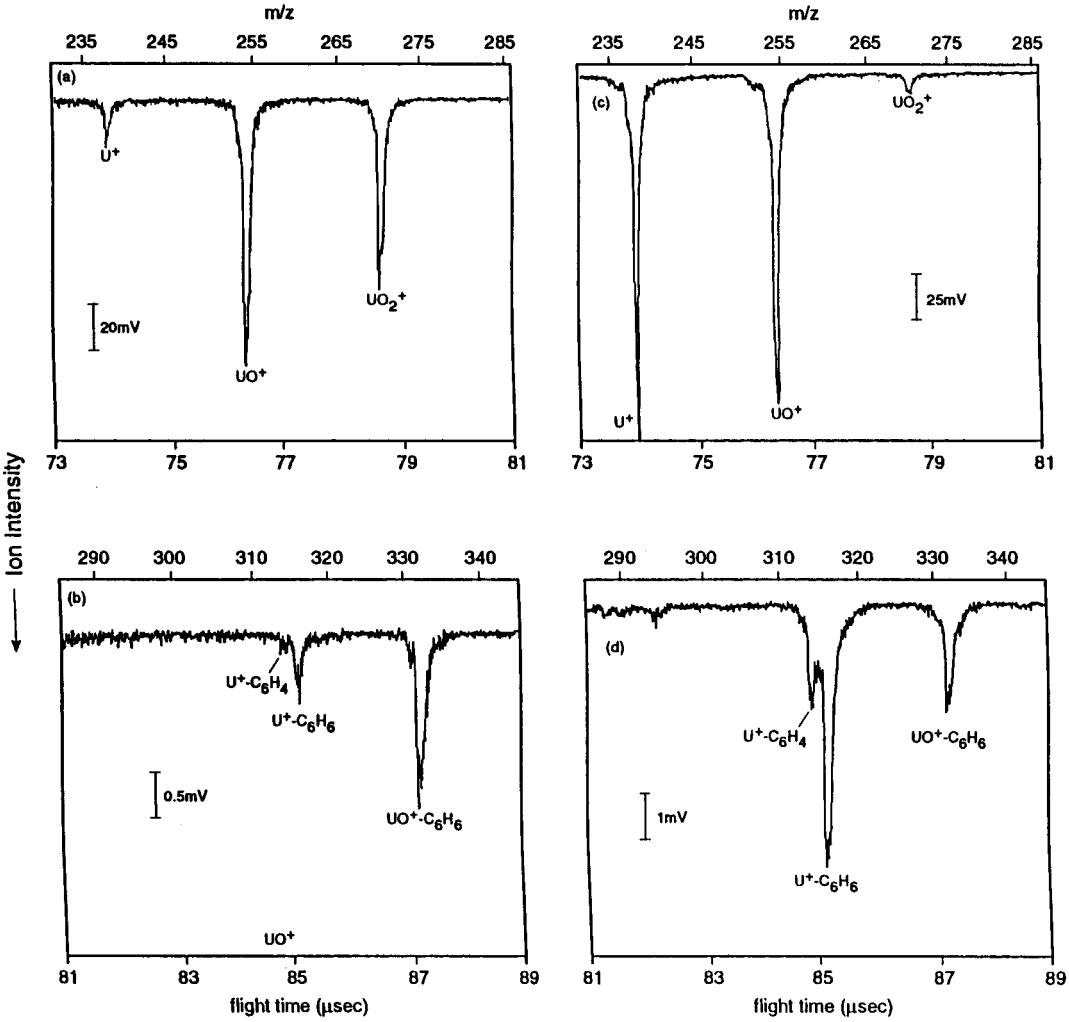

Figure 3. Mass spectra for the reaction of U^+ and UO^+ (target $\mathbf{U^o_t}$) with cyclohexene (C_6H_{10}). The spectrum in (a) and (b) was for the initial laser shots—the intense UO_2^+ peak reflects ablation of a uranium oxide surface layer. The spectrum in (c) and (d) was acquired after several hundred laser shots had removed the oxide layer.

of the exposed underlying metal—abundant U^+ and minor UO_2^+; the presence of substantial UO^+ indicates contamination of the source metal and reflects the oxophilicity of uranium.[31] It is assumed that the strong U−O bonds of ablated oxide ions remain intact during reactions with organic substrates—the observation that the yields of U^+−benzene and U^+−benzyne as a percent of U^+ were virtually invariant for these discrepant conditions confirms their derivation from parent bare U^+. The reported product yields were measured using a nearly constant ion injection delay in order to maintain comparable kinetic energy effects—similar mass species such as U^+ (238 u), UO^+ (254 u), UO_2^+ (270 u), Th^+ (232 u), and ThO^+ (248 u) would possess nearly the same energies. By varying the ion injection delay to longer times (e.g., >50 μs), lower energy ablated ions could be sampled, resulting in enhancements in the relative abundances of oxide ions compared with bare M^+. The two types of uranium metal targets (turning and wire) gave essentially the same reactivity results.

As with benzene, the results for coablated CeO_n^+, ThO_n^+, and UO_n^+ ($n = 0$ or 1, e.g., from target **CuCeTh-(U)**), reacting with cyclohexene were especially illuminating. The three naked M^+ were predictably roughly comparable regarding their efficacy in double dehydrogenation to produce the primary M^+−benzene products. Whereas both ThO^+ and UO^+ also produced

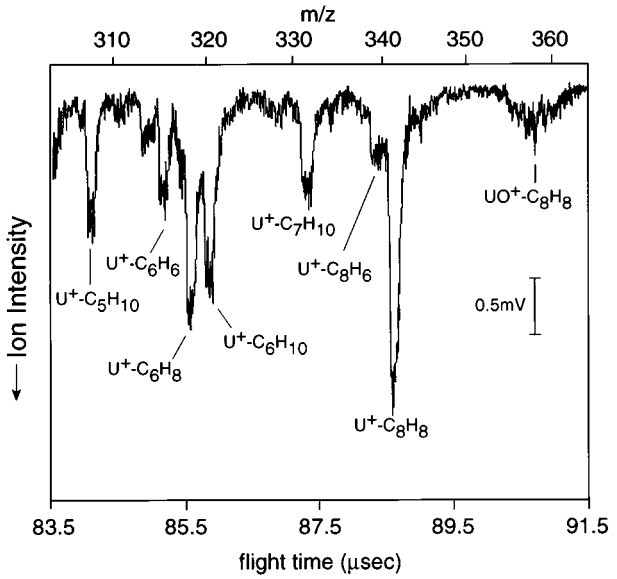

Figure 4. Portion of the mass spectrum for the reaction of U^+ and UO^+ (target $\mathbf{U^o_t}$) with 1,5-cyclooctadiene (C_8H_{12}). The intensities of U^+, UO^+, and UO_2^+ were similar to those in Figure 2 (top). The peaks designated "U^+−C_7H_{10}" and "U^+−C_5H_{10}" may be primarily UO^+−C_6H_6 and UO^+−C_4H_6, respectively.

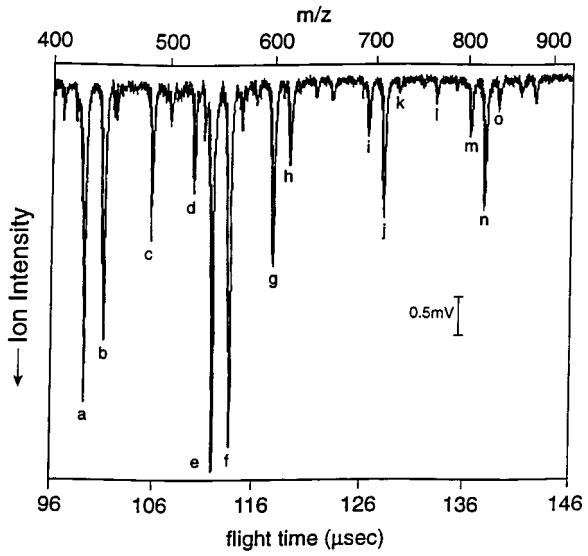

Figure 5. Portion of the mass spectrum for the ablation of the copper dispersion target **CuCeThU** into vacuum. The labeled peaks are assigned to the following metal oxide clusters: (a) $UCeO_3^+$; (b) $UCeO_3(OH)^+$; (c) $Ce_3O_4^+$; (d) $U_2O_3^+$; (e) $U_2O_4^+$; (f) $U_2O_5^+$; (g) $UCe_2O_5^+$; (h) $UCe_2O_5(OH)^+$; (i) $U_2CeO_5^+$; (j) $U_2CeO_6^+$; (k) $U_2CeO_7^+$; (l) $U_2ThO_4^+$; (m) $U_3O_6^+$; (n) $U_3O_7^+$; (o) $U_3O_8^+$.

Table 4. M^+ Excitation Energies (kJ mol^{-1})[a]

	ground	divalent	ΔE
Ce$^+$	$4f^15d^2$	ground	0
Pr$^+$	$4f^36s^1$	$4f^25d^2$	70
Sm$^+$	$4f^66s^1$	$4f^55d^16s^1$ [b]	258
Eu$^+$	$4f^76s^1$	$4f^65d^16s^1$	362
Gd$^+$	$4f^75d^16s^1$	ground	0
Tb$^+$	$4f^96s^1$	$4f^85d^16s^1$	39
Dy$^+$	$4f^{10}6s^1$	$4f^95d^16s^1$	127
Ho$^+$	$4f^{11}6s^1$	$4f^{10}5d^16s^1$ [c]	unknown
Tm$^+$	$4f^{13}6s^1$	$4f^{12}5d^16s^1$	199
Yb$^+$	$4f^{14}6s^1$	$4f^{13}5d^16s^1$	321
Lu$^+$	$4f^{14}6s^2$	$4f^{14}5d^16s^1$	142
Th$^+$	$5f^06d^27s^1$	ground	0
U$^+$	$5f^37s^2$	$5f^36d^17s^1$	3

[a] Ln^+ values from ref 36; An^+ values from ref 37. [b] Excitation energy from ground Sm^+ to the divalent $4f^55d^2$ configuration is unknown. [c] Assumes lowest divalent configuration for Ho^+ is not $4f^{10}5d^2$.

substantial MO^+−benzene, CeO^+ was apparently inert. The discrepant reactivities of LnO^+ and AnO^+ are considered below.

Products of AnO_n^+ reacting with cyclic C_8 substrates are given in Table 3. In contrast with the minor extent of An^+−benzene condensation, a primary channel for U^+ + COT was condensation as U^+−COT. As with Ln^+, the predominance of U^+−COT presumably reflects inordinately strong metal−ligand bonding. For reference, the mean metal−ligand bond dissociation energy is 347 kJ mol^{-1} for $U(COT)_2$, 247 kJ mol^{-1} for UCp_4, and substantially smaller for U−arene complexes.[12] Small amounts of the UO^+−COT and UO_2^+−COT condensation products were also identified. The dehydrogenation complexes MO_n^+−C_8H_6 and minor U^+−C_8H_4 were also formed. An intriguing observation was the formation of primarily U^+−COT condensate concurrent with primarily dehydrogenation by the monoxide to produce mainly UO^+−C_8H_6; in this case UO^+ exhibited greater C−H bond activation than did bare U^+. Similarly, ThO^+ was apparently somewhat more reactive than Th^+ while CeO^+ was contrastingly inert (see results for **CuCeTh(U)** in Table 3).

Finally, the AnO_n^+ were reacted with COD (Table 3); typical results are illustrated by the partial product ion mass spectrum for UO_n^+ + COD shown in Figure 4. The target **CuHoThU** yielded especially large yields of the UO_n^+−COD condensation product for n = 0, 1, and 2; these complexes are presumably electrostatically bonded (O_nM^+−COD). More typically, the dehydrogenation complex, MO_n^+−COT, was the dominant product. Although the results are insufficient to allow conclusive comparisons, the approximate relative reactivities of different M^+ were qualitatively consistent with other studied dehydrogenation processes. Some M^+−C_8H_6 were also evident and the efficiency of W^+ at triple dehydrogenation of COD was striking. Also footnoted in Table 3 and evident in Figure 4 are C−C activation products such as UO^+−C_6H_6.

iii. Dehydrogenation Mechanisms. Where definitive comparisons are possible, the results for dehydrogenation of C_6 and C_8 cyclic hydrocarbons by naked Ln^+, Th^+, and U^+ are consistent with the conventional model of initial insertion of a divalent metal center into a C−H bond to produce an activated C−M^+−H species which then undergoes relatively facile β-hydrogen abstraction and H_2 elimination. In particular, Ce^+, Th^+, and U^+ each have divalent ground (or very low-lying for U^+) electronic configurations and accordingly exhibit similar dehydrogenation activities. For ions such as Tb^+, some excitation energy is required to achieve a reactive divalent state (see the ΔE values in Table 4) and the overall dehydrogenation rate is correspondingly reduced. A central issue for the actinides regards the potential for direct involvement of the 5f orbitals in C−H bond activation—this would contrast with the localized and chemically passive 4f valence orbitals of the lanthanides. Since both Th^+ and U^+ possess ground or near-ground configurations with two non-5f valence electrons, their reactivities do not illuminate this issue. In contrast, Pu^+, for example, requires ~100 kJ mol^{-1} to excite to a configuration with two non-5f valence electrons[37] and determining its dehydrogenation activity should illuminate the role of valence 5f electrons in C−H bond activation.

Whereas all LnO^+ were found to be inactive at hydrocarbon dehydrogenation, both ThO^+ and UO^+ effected substantial dehydrogenation, sometimes even exhibiting greater activities than the corresponding naked An^+. The inertness of most LnO^+ is readily understood in terms of the resistance of the strong Ln−O bond to disruption,[41] and the valence saturation at the formal Ln^{3+} metal center. Among the lanthanides, Ce is the most prone to tetravalence but the single free valence electron at the metal center in CeO^+ is insufficient to promote insertion into a C−H (or C−C) bond; accordingly the inert character of CeO^+ (and other LnO^+) was predictable in the context of activation requiring oxidative addition of the metal center into a C−H bond.

Alternative routes to C−H (or C−C) bond activation by ligated metal centers involve multicenter intermediate complex species. Gas-phase examples of multicen-

(41) Chandrasekharaiah, M. S.; Gingerich, K. A. In *Handbook on the Physics and Chemistry of Rare Earths*; Gschneidner, K. A., Jr., Eyring, L., Eds.; Elsevier: New York, 1989; Vol. 12, pp 409−431.

tered activation by ions incorporating a monovalent or zero-valent metal center include C−H bond activation by $^{\bullet}Y^{+}-CH_3$ (and $^{\bullet}La^{2+}$);[30] H−H activation by $(Cp^{-})_2-Zr^{3+}-CH_3$;[42] and kinetically activated H−H cleavage by energetic ScO^+ and TiO^+, which is postulated as proceeding through a $H-M^+-O-H$ intermediate.[43]

Multicentered activation of a H−C−C−H hydrocarbon fragment by a low-valent $^{\bullet}MO^+$ (e.g., M = Ce or Th) is feasible. The more electron-rich metal center in UO^+ could affect activation by either oxidative addition into a C−H bond or by a multicentered activation process. A central question raised by the results of the present study is why ThO^+ but not CeO^+ promotes dehydrogenation. Endothermic gas-phase ion−molecule processes can be effected by kinetic activation, and some of the processes observed in this study (e.g., formation of a benzyne ligand) may require kinetic energy supplied by the ablated metal ion. The reactive ThO^+ and inert CeO^+ had the same velocities so that the kinetic energy of the more massive ThO^+ (m = 248 u) was ∼60% greater than that of CeO^+ (m = 156 u); however, the resulting kinetic energies available upon collision of ThO^+ or CeO^+ with a C_6 or C_8 hydrocarbon (m ≈ 100 u) differed by <20%,[8] presumably an insufficient discrepancy to so dramatically effect the comparative reactivities. Furthermore, CeO^+ (and other LnO^+) with substantially greater kinetic energies—studied using shorter ion sampling delays (e.g., ∼20 μs)—were also inert. It is consequently concluded that the distinctive dehydrogenation activities of ThO^+ and UO^+ compared with LnO^+ reflect intrinsic chemistry.

Among the distinctive properties of Th and U is their formation of especially strong M−H bonds,[44] possibly reflecting involvement of 5f orbitals; C−H bond activation via a C···H···M type of intermediate should presumably be enhanced by strong M−H interactions. The Ce−O, Th−O, and U−O bonds are sufficiently robust[41] to preclude oxidation processes. Theoretical treatments[45] suggest that the bonding in Ln^+-O is not fully ionic and that the bond order may exceed 2, with involvement of the oxygen "lone pair" electrons. Calculations on the bonding in ThO[46] highlighted the importance of 5f−6d hybridization which suggests a distinction from LnO and specifically CeO. A simplistic approach to evaluating the availability of the nonbonding metal center valence electron(s) in LnO^+ and AnO^+ for chemical interactions (e.g., activation) is to compare the magnitude of the energy needed to excite a 4f (Ln) or 5f (An) electron from the ground state f^n configuration of the M^{3+} to achieve a monovalent $f^{n-1}d^1$ configuration;[47] accordingly the remaining valence electron of Th^{3+} is more accessible than that of Ce^{3+}. If the 5f electrons are distinctively capable of direct involvement in C−H activation (e.g., via An−H bonding) promotion to the Th^{3+} $5f^06d^1$ or U^{3+} $5f^26d^1$ configurations would not be prerequisite to bond activation—the extreme distinction between AnO^+ and LnO^+ (multicentered) activation could be taken to suggest 5f participation without the requirement of any excitation. As indicated in Table V, the (estimated) An^{3+} f → d excitation energies continue to increase sharply beyond uranium and the reactivities of transuranic AnO^+ should serve to clarify the activation mechanism.

The extreme dependence of C−H activation by gaseous MO^+ (M = Ln or An) on the specific identity of M indicates pivotal involvement of the metal center. The following simplified activation process for the example of ThO^+ + cyclohexene is postulated by analogy with that proposed for solid metal oxide and gaseous SO_2 catalyzed *cis*−*trans* isomerization of 2-butene:[48]

$$O{=}Th^+ + -CH{=}CH-CH_2-CH_2- \text{ (in } C_6 \text{ ring)} \quad (2a)$$

$$\downarrow$$

$$H-O-Th^+\text{-}\pi\text{-}\{\eta^3\text{-}CH-CH-CH-\}-CH_2- \quad (2b)$$

$$\downarrow$$

$$O{=}Th^+\text{-}\pi\text{-}\{-CH{=}CH-CH{=}CH-\} + H_2 \quad (2c)$$

The postulated intermediate in eq 2b comprises a metal center π-bonded to the η^3-allylic π-delocalized anionic moiety (incorporated in a C_6 ring). The speculated participation of 5f orbitals in organometallic π-bonding in complexes such as that in eq 2b could account for the greater dehydrogenation activity of ThO^+ compared with CeO^+.

iv. Metal Oxide Clusters. Previous results from our laboratory[34] demonstrated the synthesis of lanthanide oxide clusters by direct laser ablation into vacuum of hydrated complex oxide solids such as oxalates. Similarly, in the course of the present investigation, uranium oxide clusters were produced during ablation into vacuum of the **CuCeThU** target which comprised hydrated uranyl acetate; the observed cluster formation for this minor constituent (2 at. % U) demonstrates the oxophilicity of uranium. A vacuum ablation mass spectrum showing several U-containing metal oxide clusters is shown in Figure 5. The cluster ion intensities (note vertical millivolt scale in Figure 5) compare with the following approximate intensities for the coablated primary species: Ce^+/1 mV; CeO^+/50 mV; U^+/3 mV; UO^+/50 mV; UO_2^+/100 mV; ThO^+/2 mV. The relative dearth of ablated ThO^+ was typical (Th^+ was even less abundant); it is presumed that thorium was ablated primarily as neutral species, probably ThO and/or ThO_2.

Uranium exhibits a very complex oxide chemistry in the solid state which reflects the availability of several oxidation states.[32] Gas-phase uranium oxide clusters exhibiting multiple uranium valence states were reported for ablation of solid UO_2 under conditions similar to those used here.[33] It is instructive to assign formal metal site valences in these oxide clusters. Based upon previous results[34] and the appearance here of $Ce_3O_4^+$—in which all Ce are trivalent—as the only binary Ce−O cluster, Ce is consistently assigned a primary valence of +3 (although Ce^{4+} is feasible). The clusters in Figure 5 are then designated with the following valence distributions by assuming all oxygens are as O^{2-} and that

(42) Christ, C. S.; Eyler, J. R.; Richardson, D. E. *J. Am. Chem. Soc.* **1988**, *110*, 4038−4039.
(43) Clemmer, D. E.; Aristov, N.; Armentrout, P. B. *J. Phys. Chem.* **1993**, *97*, 544−552.
(44) Jemine, X.; Goffart, J.; Berthet, J.; Ephritikhine, M. *J. Chem. Soc., Dalton Trans.* **1992**, 2439−2440.
(45) Tilson, J. L.; Harrison, J. F. *J. Phys. Chem.* **1991**, *95*, 5097−5103.
(46) Marian, C. M.; Wahlgren, U.; Gropen, O.; Pyykko, P. *J. Mol. Struct. (THEOCHEM)* **1988**, *169*, 339−354.
(47) Brewer, L. *J. Opt. Soc. Am.* **1971**, *61*, 1666−1682.
(48) Rooney, J. J. *J. Mol. Catal.* **1985**, *31*, 147−159.

the +1 net ion charge resides on a metal site: (a) U^{4+}-$Ce^{3+}O_3$; (b) $U^{5+}Ce^{3+}O_3(OH)$; (c) $Ce^{3+}{}_3O_4$; (d) $U^{3+}U^{4+}O_3$; (e) $\mathbf{U^{4+}U^{5+}O_4}$; (f) $U^{5+}U^{6+}O_5$; (g) $U^{5+}Ce^{3+}{}_2O_5$; (h) U^{6+}-$Ce^{3+}{}_2O_5(OH)$; (i) $U^{4+}{}_2Ce^{3+}O_5$; (j) $U^{5+}{}_2Ce^{3+}O_6$; (k) $U^{6+}{}_2$-$Ce^{3+}O_7$; (l) $U^{3+}{}_2Th^{3+}O_4$; (m) $U_2{}^{4+}U^{5+}O_6$; (n) $\mathbf{U^{5+}{}_3O_7}$; (o) $U^{5+}U_2{}^{6+}O_8{}^+$. The principal binary uranium oxide clusters (designated in bold) suggest dominance of U^{5+}, which accords with the concurrent abundance of elementary $UO_2{}^+$ ($\sim U^{5+}O^{2-}{}_2$). Although similar binary U−O clusters were reported for UO_2 ablation,[33] the cluster abundance distributions there indicated somewhat less oxidizing conditions—UO^+, $U_2O_3{}^+$, and $U_3O_6{}^+$ were the dominant species. Clusters such as those identified here are of intrinsic interest, particularly for the actinide elements where multiple and variable oxidation states may be manifested.

Conclusions

Several representative Ln^+ ions were reacted with cyclic C_8 hydrocarbons of varying degrees of saturation. Reaction with COT resulted in a substantially greater yield of the condensation product than was found under similar conditions with benzene; this distinction is attributed to the particularly strong organolanthanide bonding in the condensation adduct, Ln^+−COT. Large variations were determined in the effectiveness of different Ln^+ at dehydrogenation of C_8 hydrocarbons. The revealed reactivity trends were consistent with those found previously for comparable reactions with cyclic C_6 hydrocarbons and are interpreted to indicate an initial rate-controlling step of insertion of a divalent Ln^+ into a C−H bond, presumably followed by relatively facile β-H abstraction and ultimately H_2 elimination. Specifically, the relative Ln^+ reactivities closely parallel the magnitude of the energy necessary to excite the ground state Ln^+ to a divalent configuration with two non-f valence electrons available for bonding in a C−Ln^+−H activated complex.

The early actinide ions, Th^+ and U^+, were reacted with both cyclic C_6 and C_8 hydrocarbons. The results were similar to those found for Ln^+ with the dehydrogenation activities of these An^+ roughly comparable to that of the most reactive lanthanide, Ce^+. The high An^+ reactivities are consistent with the requirement of two valence electrons for C−H activation since the ground state of Th^+ is divalent and U^+ has a divalent excited state only 0.03 eV above ground. The availability of An^+ configurations with two valence electrons in non-5f orbitals precludes characterizing the ability of 5f electrons to directly participate in C−H bond activation; studies with transuranium actinides are needed to address this central issue. The facile preparation of gaseous An^+−COT and An^+−arene demonstrates the ability to prepare fragile organoactinide species whose condensed-phase counterparts may be insufficiently durable to study by conventional condensed-phase techniques. For example, the L−U^{III}−COT analogs of gaseous U^+−COT can be prepared only under extreme conditions and few U−arene complexes have been isolated.

The most striking distinction between the observed gas-phase organolanthanide and organoactinide chemistries was the substantial AnO^+ reactivities in contrast to virtually inert LnO^+. Most notably, CeO^+ was inert whereas ordinarily similar ThO^+ was an effective dehydrogenation agent. The mechanism of C−H activation by ThO^+, and possibly UO^+, probably involves a multicentered activated complex. The distinctive reactivity of ThO^+ may reflect the availability of a relatively low-lying monovalent configuration for Th^{3+} or possibly direct participation of 5f electrons in C−H activation via An−H interactions. The central underlying role of relativistic effects in actinide chemistry—particularly organoactinide chemistry—is increasingly well-established,[49] and it is probable that the apparently unique behaviors of ThO^+ and UO^+ revealed in the present study have relativistic underpinnings.

An ancillary result of the present study was the identification of several metal oxide clusters comprising uranium. The stoichiometries of these clusters reflect the complex chemistry of uranium and reveal coexisting oxidation states. It would be illuminating to characterize reactivities of such oxide clusters with organic molecules for comparison with elementary ion−molecule reactions and catalytic processes occurring at the gas−solid interface.

Acknowledgment. This work was sponsored by the Division of Chemical Sciences, Office of Basic Energy Sciences, U.S. Department of Energy, under Contract DE-AC05-96OR22464 at Oak Ridge National Laboratory with Lockheed Martin Energy Research Corp.

OM970205P

(49) Kaltsoyannis, N. *J. Chem. Soc., Dalton Trans.* **1997**, 1−11.